

EfficientRainNet: Smaller Neural Networks Based on EfficientNetV2 for Rainfall Nowcasting

Muhammed Sit^{a,*}, Bong-Chul Seo^a, Bekir Demiray^a, Ibrahim Demir^{a,b,c}

^a IIHR Hydrosience and Engineering, University of Iowa, Iowa City, Iowa, USA

^b Civil and Environmental Engineering, University of Iowa, Iowa City, Iowa, USA

^c Electrical and Computer Engineering, University of Iowa, Iowa City, Iowa, USA

* Corresponding Author, Email: muhammed-sit@uiowa.edu

Abstract

Rainfall nowcasting provides short-term, high-resolution information on the location, intensity, and timing of rainfall, which is crucial for weather forecasting, flood warning, and emergency response. This can help people and organizations make informed decisions to mitigate the impact of severe weather events and reduce the risk of damage and loss of life. There are many attempts at tackling the problem at hand, whether it be numerical models or statistical models that also comprise deep neural networks. Even though nowcast models are quite accurate nowadays and the problem has a saturated literature, current approaches mostly focus on improving the nowcast performance while the computational burden keeps increasing. In this study, we propose EfficientRainNet, which is a convolutional neural network architecture that is based on mobile inverted residual linear bottleneck blocks with a few alterations. We show that EfficientRainNet is able to produce comparable results to those of encoder-decoder convolutional GRUs with only a fraction of the trainable parameters over a radar rainfall dataset for the State of Iowa. Also, for the most part, EfficientRainNet performs better than baselines using persistence- and optical flow-based nowcasting, along with another computational efficiency-focused neural network architecture, Small Attention UNet.

This manuscript is an EarthArXiv preprint that is not peer-reviewed or submitted to a journal. Subsequent versions of this manuscript may have slightly different content. Please feel free to contact the corresponding author for feedback.

1. Introduction

Nowcasting rainfall has been an important task to address as rainfall affects many aspects of human life on earth extensively for planning (Yildirim et al., 2022), mitigating (Alabbad and Demir, 2022), and responding to a wide range of natural hazards (Teague et al., 2021). The current state of the art for rainfall nowcasts requires huge computational power and resources to run numerical weather prediction (NWP) models operationally in real-time. NWP models are based on complex mathematical equations that take into account physical features of weather such as air motion, humidity, and pressure and are costly to operate. NWP models typically generate forecasts ranging from a few hours to weeks. In a changing climate, the frequency and severity of severe precipitation events are projected to rise (Davenport et al., 2021). This projection makes it more important to forecast precipitation accurately to support mitigation decisions (Montz and Grunfest, 2002; Ewing and Demir, 2021), flood risk assessment (Warner and Cranston, 2009; Yildirim and Demir, 2022), and planning and response efforts (Cools et al., 2016; Alabbad et al., 2022). Current atmospheric models like High-Resolution Rapid Refresh (HRRR) by the National Oceanic and Atmospheric Administration (NOAA) are critical for forecasting precipitation, but they lack when it comes to short-term forecasts or nowcasts.

Nowcasting rainfall refers to forecasting rainfall for short ranges (0–6 hours) using radar echo maps (Hering et al., 2004) and has been a topic of interest beyond model-driven approaches from the atmospheric sciences as NWP models are costly to operate both in terms of time and resources. Data-driven approaches to the problem of nowcasting rainfall start with relatively simple workflows. One of these approaches that does not rely on extensive atmospheric information is based on optical flow calculations, but such an approach does not take into account the complex characteristics that cloud movements manifest through their activity. For this very reason and to take advantage of the abundance of measured radar rainfall products, artificial neural network models have been utilized. The complexity of these models varies, starting with more conventional machine learning models and progressing to increasingly complex ones that employ many state-of-the-art approaches from the deep learning literature.

Nowcasting has been extensively studied using deep learning, and the field is somewhat saturated for approaches that only use time-series of historical radar rainfall data. As seen in related work, one thing that comes into prominence in the field is the fact that approaches have become increasingly complex, requiring more and more computational resources based on exponentially more trainable parameters while offering relatively smaller progress.

Workloads worsen the memory bottleneck that lowers the overall performance of systems where deep learning models are run since neural network workloads continue to have big memory footprints and significant computational requirements to attain improved accuracy (Inci 2022; Inci et al., 2022a). As deep learning models have become more proficient in many tasks, developing smaller neural network models in terms of trainable parameters has attracted interest from many researchers in the field (Inci et al., 2022b) to support operational needs in flood forecasting (Krajewski et al., 2021; Xiang and Demir, 2022) and inundation mapping (Hu and Demir, 2021; Li et al., 2022).

While it is true that certain tasks have been shifted to mobile devices to streamline operational processes, it is essential to note that these devices are often less powerful than traditional development or experimentation environments. To optimize performance, it is crucial to prioritize lower memory usage, energy efficiency, and faster model execution, particularly for complex tasks such as rainfall forecasting or nowcasting. Beyond energy-efficient neural network training for cost-cutting purposes only, there have been efforts to move environmental monitoring and modeling efforts to edge devices or serverless environments (Hu et al., 2019) for faster decision-making and easier access to environmental data. However, because of the strict performance per area and energy limitations of the edge devices, the growing size and computational cost of environmental models have become a challenging task for on-device machine learning endeavors.

In this study, we present a novel deep neural network model, EfficientRainNet, for rainfall nowcasting for up to 2 hours with a 10-minute temporal resolution and a case study in Iowa to improve the efficiency of the rainfall nowcasting models with less power and memory needs. The EfficientRainNet model is broadly based on EfficientNetV2 (Tan and Le, 2021), which is based on MobileNetV2 (Sandler et al., 2018). EfficientNetV2 utilizes mobile inverted bottleneck convolutions (MBConv). The MBConvs in this study were slightly altered and used in an encoder-decoder fashion. EfficientRainNet was compared to persistence and dense optical flow-based baselines using rainfall nowcast metrics from the literature. Also, in order to evaluate the performance of the EfficientRainNet while using drastically less memory, the results of the small attention UNet (SmAt-UNet) (Trebing et al., 2021), which were also developed with rainfall nowcasting in mind, and encoder-decoder ConvGRUs (Shi et al., 2017), will be presented. To show the performance of the proposed model against a more traditional approach, the performances of EfficientRainNet and HRRR will be shared side-by-side where data availability allows within the test dataset timeframe.

The remainder of this paper will be structured as follows: in the following section, related work will be shared, first describing the literature on rainfall forecasting and then briefly painting a picture of energy-aware deep learning efforts. Following that, the methodology will be defined, starting with the details of EfficientRainNet, baseline neural network models from the literature, and then other more conventional baselines. Then, in Section 4, the experiments will be defined with the dataset at hand, followed by the results of those experiments in Section 5. Finally, in Section 6, conclusions and future plans will be presented.

2. Related Work

2.1. Rainfall Nowcasting with Deep Learning

Literature on precipitation nowcasting could be categorized by the methodologies employed. Physically-based atmospheric modeling and statistical modeling are two methodological approaches that are widely employed by researchers. Along with technological advancements for tensor computations with graphics processing units, as is the case with many subdisciplines in the water field (Sit et al., 2020), utilization of artificial neural networks has seen a spike in

nowcasting as well as many application areas in earth and climate studies for data augmentation (Demiray et al., 2021), synthetic data generation (Gautam et al., 2021), and forecasting tasks

Forecasting rainfall is typically done in a fashion where the product is a 2D tensor or a set of 2D tensors of estimated precipitation for a gridded area. Since a matrix is produced at the end, the task at hand is quite similar to a video frame prediction task. Therefore, beyond rainfall forecasting, the prediction of 2D tensors has been an important problem to investigate among computer vision researchers for video frame prediction.

Convolutional LSTMs are the starting point for 2D precipitation forecasting (ConvLSTMs) using deep learning. ConvLSTMs were suggested for use in the process of radar echo forecasting by Shi et al. (2015). The researchers fed the network five frames of data totaling thirty minutes and trained it to predict fifteen frames over the course of one and a half hours. They compared their findings to a technique known as ROVER, which is an extrapolation method. Shi et al. (2017) proposed Trajectory GRU (TrajGRU), which is an encoder-decoder architecture where the input frames go through a series of downsampling and recurrent neural network (RNN) layers in the encoder part, then go through a series of RNN and upsampling layers in the decoder (namely the forecaster) part to finally output the forecasts. This improves what ConvLSTMs achieve.

TrajGRU was evaluated on the HKO-7 radar echo dataset for Hong Kong as well as Moving MNIST, and it was demonstrated to be superior to ConvLSTM, ConvGRU, 2D CNNs, and 3D CNNs. TrajGRUs were presented with the intention of giving an alternative that is location-variant as opposed to the location-invariant ConvRNNs. Furthermore, Shi et al. (2018) came up with the idea of Recurrent Dynamic CNNs (RDCNN). RDCNN is comprised of a recurrent dynamic sub-network and a probability prediction layer. These two layers work together to produce a cyclic structure in the convolution layer, which improves the network's ability to handle time-related frames. Case studies used radar data from Nanjing, Hangzhou, and Xiamen, China.

Jing et al. (2019) presented Multi-Level Correlation Long Short-Term Memory (MLC-LSTM) that takes advantage of adversarial training. Following the construction of an encoder-predictor architecture for end-to-end radar echo extrapolation based on the MLC-LSTM, they utilize a CNN as the discriminator. The training of the networks included both image loss and adversarial loss, which resulted in an extrapolation of radar echoes that were more realistic and fine-grained. Luo et al. (2020) developed a new pseudo-flow spatiotemporal LSTM unit (PFST-LSTM), which integrates a spatial memory cell and a position alignment module into the LSTM. They tested PFST-LSTM units for 2D forecasting over the Moving MNIST dataset, which demonstrated that the design can effectively incorporate information regarding spatial appearances and velocities. In addition to this, they demonstrated that PFST-LSTM outperformed TrajGRU and other 2D forecasting architectures derived from non-radar echo-forecasting literature, such as PredRNN (Wang et al., 2017) and ST-LSTM (Tang et al., 2019).

Cao et al. (2019) proposed using an RNN as the foundation for a star-bridge network (StarBriNet). The model consists of multiple sub-networks, each of which is designed to handle a

certain range of rainfall intensities and durations. In addition to this, they developed a star-shaped information bridge with the purpose of enhancing the flow of data between the RNN layers. The networks were trained with a multi-sigmoid loss function so that they could properly take into consideration the precipitation nowcasting. They compared their method to the ConvLSTM and Conv3D approaches for a resolution of 6 minutes.

Xie et al. (2020) suggested an energy-based GAN called EBAD. The discriminator produces low energy for real data and high energy for produced data. The generator is based on ST-LSTM. Over the region of Guangdong, China, the authors evaluated EBAD in comparison to ConvGRUs, generative adversarial ConvGRUs, and optical flow. The concept of spatiotemporal convolutional long short-term memory (ST-ConvLSTM) was proposed by Zhong et al. (2020). This model makes use of the attention mechanism to mimic long-range and long-term spatiotemporal dependence and makes use of ConvLSTM to collect coarse spatiotemporal information. The authors evaluated their method in comparison to ConvLSTM, ConvRNN, and PredRNN, as well as the ConvGRU version of the suggested architecture, which was described as ST-ConvGRU over Moving MNIST and radar echoes for Guangzhou, China.

In a converse attempt that does not utilize RNNs, a CNN called RainNet was proposed by Ayzel et al. (2020) for radar-based precipitation nowcasting. The U-Net (Ronneberger et al., 2015) and SegNet (Badrinarayanan et al., 2017) models, which were first developed for the purpose of addressing binary segmentation issues, served as the impetus for the development of the RainNet. RainNet was trained to estimate continuous precipitation intensities with a 5-minute lead time using weather radar data for Germany that was collected over the course of several years and subjected to quality control. In order to achieve a lead time of one hour, a recursive method was used. This method utilized forecasts made at lead times of five minutes as model inputs for lead periods of one hour and beyond. Both persistence, which implies that the prediction is the same as the last known frame, and Rainymotion, which is an optical flow-based 2D forecast library, were evaluated alongside this method in order to determine which was superior.

MetNet is an architecture that was presented by Sønderby et al. (2020) and driven by ConvLSTM that provides accurate forecasts that extend for up to eight hours across an area that is one kilometer by one kilometer. The data were collected at a resolution of 2 minutes for the continental United States. MetNet is able to create probabilistic precipitation maps utilizing radar and satellite data as well as forecast lead time, which allows it to surpass the HRRR method. MetNet was upgraded by Espeholt et al. (2021) and provided as MetNet-2. This was accomplished by incorporating cumulative rainfall data from rain gauges. Both of these methods use more than just radar echoes in forecasts.

A fusion module was proposed for RainfallNet (Huang et al., 2021). In this module, similar to the fashion MetNet and MetNet-2 employ, radar echo observations and numerical weather prediction (NWP) data would be combined. The architecture is made up of three different components: (1) dual encoders for extracting spatio-temporal features from radar echo images and NWP data; (2) combining channel and spatial attention; and (3) a loss function that

combines structural similarity loss, mean square error, and mean absolute error with different weights for each rainfall level in order to further increase the sensitivity. They compared RainfallNet against other models, such as TrajGRU, ConvLSTM, and PredRNN++ (Wang et al., 2018), which is an upgraded version of PredRNN.

Flow-Deformation Network (FDNet) is a neural network that was introduced by Yan et al. (2021). This network is able to forecast flow and deformation in two parallel cross paths. In order to efficiently handle the complicated and highly non-stationary evolution of radar echoes, FDNet suggested breaking down the movement into optical flow field motion and morphologic deformation. The deformation encoder is able to determine a change in shape based on the translational motion of radar echoes, whereas the flow encoder is able to determine motion in the optical flow field between two successive frames. The authors contrasted the performance of the FDNet with that of the ConvLSTM and other state-of-the-art methods like TrajGRU. In a more hybrid approach, MS-nowcasting was presented by Kloczek et al. (2021), and it is an encoder-decoder ConvLSTM architecture that allows atmospheric models such as HRRR to be included in the process. The authors demonstrated that variants of the suggested model that were combined with atmospheric models performed significantly better than the original variant in both the United States and Europe.

Interactional Dual Attention Long Short-term Memory, or IDA-LSTM, is a neural network architecture for nowcasting that was proposed by Luo et al. (2021). Their concept included (1) an interaction scheme between the hidden state and the input of LSTMs and (2) a dual attention module for both channel and temporal information. The goal of this concept was to improve long-term spatiotemporal recognition. IDA-LSTM incorporated both of these concepts. They compared IDA-LSTM to ConvLSTM, ConvGRU, TrajGRU, PredRNN, and PredRNN++, along with some other models from the literature, using the data from the CIKM AnalytiCup 2017. In a different strategy, Luo et al. (2021) suggested integrating a Region Attention Block (RAB) into ConvRNNs in order to improve weather forecasting in regions that experience high levels of precipitation, namely RAP-Net. They also presented the Recall Attention Mechanism (RAM) in order to make the prediction more accurate. By preserving information over longer periods of time, RAM makes predicting more accurate. The results of their experiments demonstrated that RAP-Net performed significantly better than a variety of state-of-the-art architectures, including TrajGRU and PFST-LSTM, amongst others.

As this literature summary suggests, most of the studies on rainfall nowcasting focus on improving the forecasts in terms of metrics, while the efficiency of the proposed models is more often than not simply overlooked. One exception to this trend is Small Attention U-Net (Trebing et al., 2021), where U-Net is broadly compressed by replacing regular 3x3 convolutions with 3x3 depthwise separable convolutions. Beyond this point, they also introduce attention mechanisms to UNet that, in turn, improve forecasting performance.

2.2. Energy Efficient Deep Learning

Even though energy-efficient deep learning has less momentum than application research, there have been many efforts to overcome memory and computational power limitations. To achieve this, system architects research hardware architectures to solve the memory bottleneck issue and enhance system performance (Chen et al., 2016; Aly et al., 2015; Han et al., 2016), while deep learning practitioners concentrate on model compression (Han et al., 2015; Ding et al., 2018; Chin et al., 2020) techniques. Since this study focuses on designing a relatively small but performance-wise comparable method, the literature on more efficient deep learning models will be briefly covered here.

As is the case with pioneering deep learning architectures for image recognition, the effort for compressed deep learning models has been around since the ImageNet competition to develop models with better scores. Many researchers have found the motivation to build smaller networks since state-of-the-art neural network architectures were working with millions of parameters. Although it still has the utmost importance to advance the state-of-the-art in terms of the final performance, advancing in a practical direction also attracts attention from researchers.

For this very reason, there have been attempts to compress deep learning models with a tradeoff where efficiency is preferred over accuracy. Scaled ResNets (He et al., 2016) such as ResNet18 or ResNet200 could be mentioned, to name a few. For practical purposes, focusing on the performance over the ImageNet dataset, there have been studies that present scaled-down convolutional neural networks that perform similarly to the state of the art. Considering there have been many attempts at improving nowcasting performance using deep learning that has increasingly complex architectures, it is worth exploring ways to build architectures that are capable of nowcasting while requiring less computational resources.

MobileNet with mobile inverted bottleneck convolutions and later, borrowing the methodology from MobileNet, EfficientNet shows that smaller convolutional networks could achieve at least comparable performance over widely used datasets. In the nowcasting literature, SmAt-UNet and STConvS2S (Castro et al., 2021) could be named as attempts at presenting smaller but efficient neural networks.

In a similar fashion, this study explores the capability of mobile inverted bottleneck convolutions (MBConv) in rainfall nowcasting to provide a step towards more efficient deep learning-based rainfall forecasts. In order to show that, an MBConv-based neural network that will be referred to as EfficientRainNet in this paper will be compared to the baselines of an optical flow-based advection-correction method and persistence. To see whether EfficientRainNet provides comparable results, a slightly upscaled version of Encoder-Decoder ConvGRU proposed in Shi et al. (2017) that was upscaled so that the spatial resolution of the data used in this paper could be subsumed and SmAt-UNet will be employed. Finally, EfficientRainNet will also be compared to HRRR where data limitations allow.

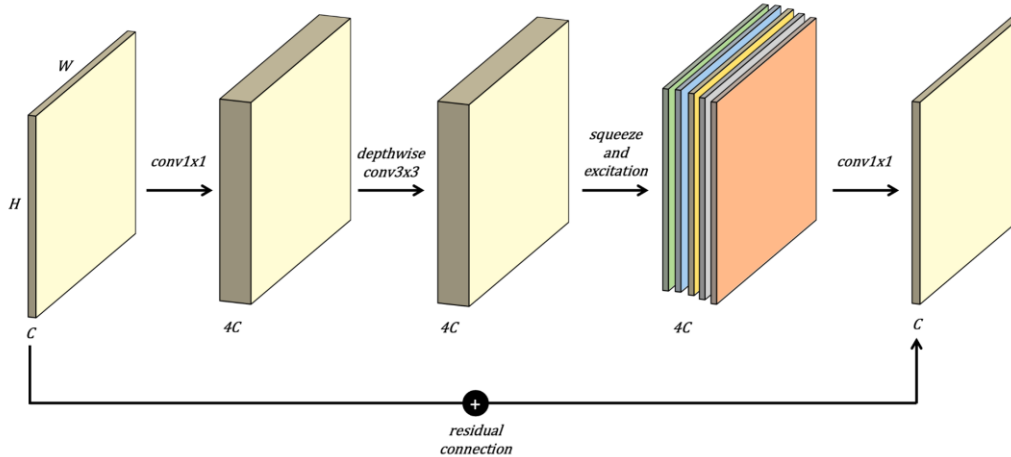


Figure 1. MBConv block architecture and connections

3. Methodology

3.1. EfficientRainNet

EfficientRainNet is based on the MBConv blocks (Figure 1) that were introduced in EfficientNetV2. An MBConv block is principally the same as an inverted residual linear bottleneck block (Figure 2), which was inspired by the residual bottleneck block (Figure 3) from the original ResNet. Inverted residual linear bottleneck blocks and residual bottleneck blocks have three differences: (1) using depthwise convolutions instead of regular convolutions; (2) utilizing linear bottlenecks as opposed to non-linear bottlenecks; and (3) inverted residual connections.

Depthwise Convolutions: While a residual bottleneck block uses regular convolutions throughout the block, in an inverted residual linear bottleneck block, a depthwise convolution is used where using a regular convolution comes with drastically more computation time and memory along with regular convolutions. By using a single convolutional filter for each input feature map, a depthwise convolution layer performs minimal filtering. Contrarily, a regular convolution employs as many filters as desired that are shared among feature maps.

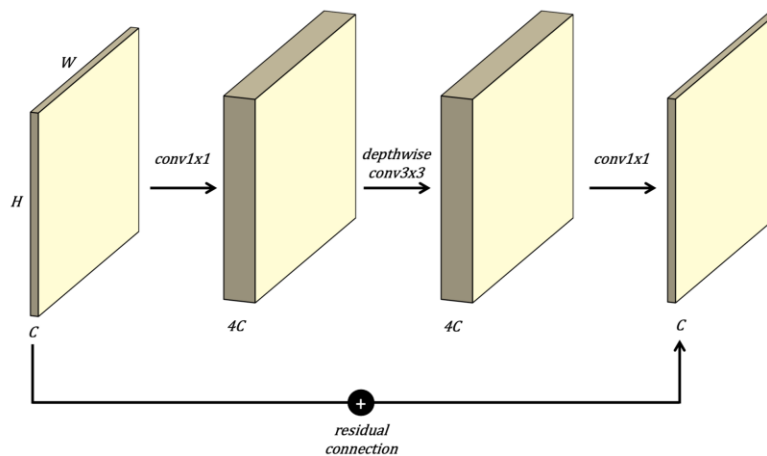


Figure 2. Inverted Residual Non-linear Bottleneck Block architecture and connections

Linear Bottleneck: The original bottleneck block is non-linear. The non-linearity is ensured by a non-linear activation function, which is typically the ReLU function. As opposed to that, there is no activation at the end of the inverted residual non-linear bottleneck block. According to experimental data, using linear layers is essential because it stops non-linearities from destroying too much information.

Inverted Residuals: Residual blocks have the residual connection between layers with high-dimensional layers, whereas inverted residual non-linear bottleneck blocks do the opposite. The residual connection is between low-dimensional layers that have the dimensional expansion between them, hence the name "inverted." In other words, while the original residual bottleneck block goes in a wide-narrow-wide fashion, the inverted residual non-linear bottleneck block goes narrow-wide-narrow. MobileNetv2 authors have shown that this approach increases performance and is more memory efficient.

While inverted residual non-linear bottleneck blocks prove more efficient, there is still room for improvement. The authors of EfficientNetV2 demonstrate that by expanding the block with attention and presenting MBConv, MBConv utilizes a squeeze and excitation layer (SE Layer) (Hu et al., 2018) (Figure 4) to facilitate attention. The SE layer is placed right before the last convolution layer in the block.

The SE Layer works on the premise that each channel (or feature map) in an input might have different importance for the outcome. With this premise, the idea becomes to train a set of weights that has the same length as the number of channels in the input. To enable this, in an SE layer, the input is first average-pooled into a vector, which is called the "squeeze" operation. Following the squeeze operation, the vector is fed through a set of fully connected (or convolutional) layers, and a vector with weights is produced. Finally, the weight vector, which is the output of the fully connected layers, is used to "excite" the original input.

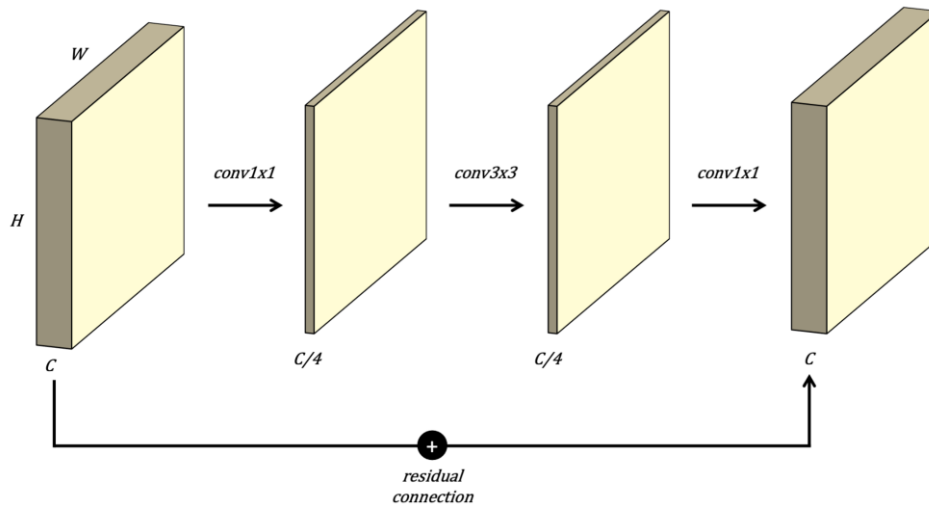


Figure 3. Residual bottleneck architecture and connections

Inverted residual non-linear bottleneck blocks provide an economical residual block by replacing costly convolutions with less costly depthwise convolutions. Later, taking advantage of the SE layer, the MBConv is shown to perform better than its predecessor in image classification tasks, thus presenting a viable candidate for any efficient neural network design that would potentially need convolutions. In this paper, we employ MBConv as the main building block of the EfficientRainNet, with two differences: 1) the batch normalization that was used after each convolution layer is removed, and 2) the swish function is replaced with LeakyReLU, as we've empirically seen these alterations change the performance over rainfall data in a different direction, which will be discussed later.

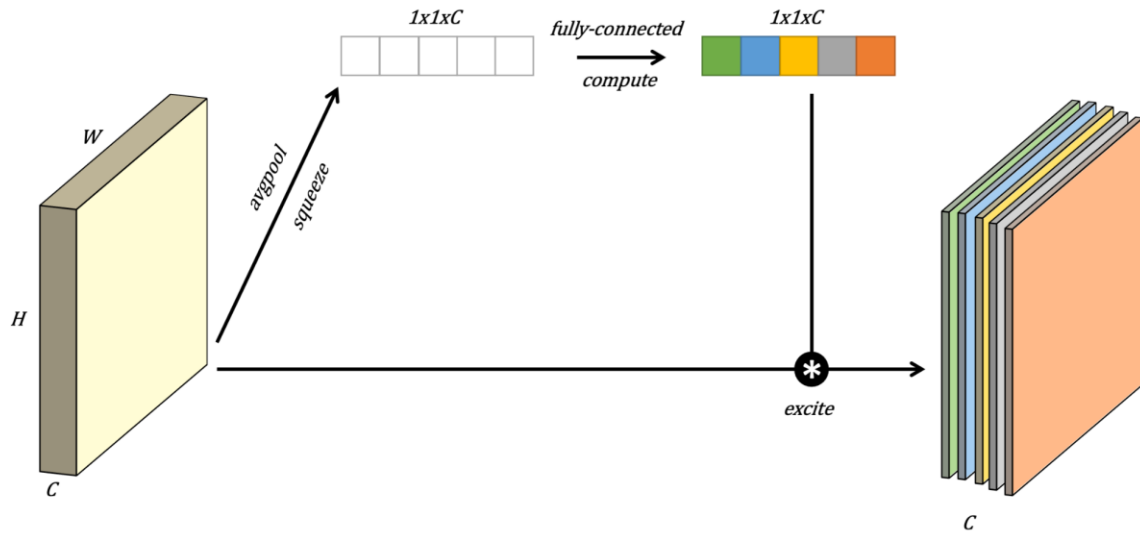


Figure 4. Squeeze-and-Excitation layer architecture and connections

Figure 5 depicts the EfficientRainNet architecture created by stacking MBConv blocks. More often than not, to ensure an optimal training process, the number of feature maps is chosen to be divisible by 8. Following this rule of thumb, the MBConv input and output numbers of feature maps are chosen to be divisible by 8. However, since the number of time steps for the task at hand is 12, a convolution layer is used as an encoder before the input is fed through MBConv layers.

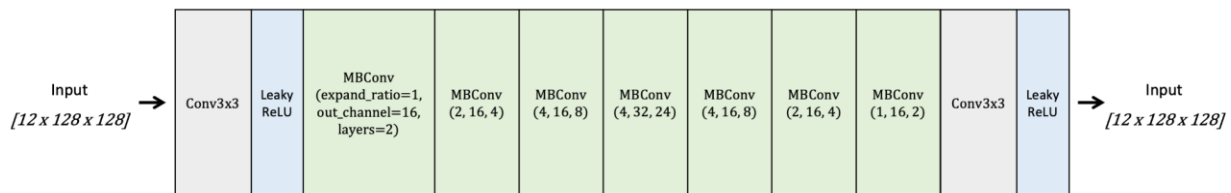


Figure 5. EfficientRainNet architecture and connections

Table 1. Trainable parameters of each of the neural networks employed in this study. The best score is highlighted in **bold**; the second best is underlined.

Algorithms	Model Size ▼	Model Ratio ▼
ConvGRU	6,880,289	1.000x
SmAt-UNet	<u>4,034,252</u>	<u>0.590x</u>
EfficientRainNet	358,800	0.052x

3.2. Comparison Models

The performance of EfficientRainNet will be compared to selected deep learning models from the rainfall nowcasting literature to show its effectiveness.

3.2.1. Encoder-Decoder ConvGRUs

As specified in the literature review, nowcasting with deep learning starts with Convolutional Long Short-term Memory (ConvLSTM) networks, or, shortly, ConvLSTMs (Shi et al., 2015). Later, in a more specific version of the approach, authors present Convolutional Gated Recurrent Unit (ConvGRU) networks along with an encoder-decoder architecture where both ConvLSTMs and ConvGRUs are utilized (Shi et al., 2017). In both of these networks, the main idea is to replace matrix multiplications within the recurrent node with convolution operations so that an input that is higher-dimensional than a vector could go through the node without loss of dimensionality. Encoder-Decoder ConvGRUs utilize ConvGRUs along with convolutional layers and activations to first encode the input time series rainfall maps and then decode the forecasts with the decoder. One limitation of the encoder-decoder ConvGRUs is that the sequence length for the output needs to match that of the input. Since it states one of the major steps towards precipitation nowcasting with deep learning, the performance of the EfficientRainNet that this paper presents will be compared to the performance of the encoder-decoder ConvGRU networks, which will be referred to as ConvGRUs throughout this paper.

For the details of the formulation and the details of the encoder-decoder ConvGRUs, we suggest the reader refer to the paper. Note that the only difference between the neural network architecture in Shi et al. (2017) and the ConvGRU network used in this study is about the size of the rainfall maps. Our data is 128x128 in size, whereas the data used in that study is 64x64. So, to ensure proper downscaling and upscaling, the input sizes for ConvGRU layers within both the encoder and the decoder are changed to be the double of the original in the paper.

3.2.2. Small Attention UNet (SmAt-UNet)

Small Attention UNet (SmAt-UNet) (Trebing et al., 2021) is a variation of UNet. Even though UNet was designed for image segmentation tasks, there are many applications of UNet for various purposes. Since UNet is built in a fashion where both the input and output are matrices, which could be of the same shape, and optionally with many channels, it is possible to use UNet for nowcasting right off the bat. However, the number of parameters for UNet does not justify the performance in nowcasting. Consequently, authors propose SmAt-UNet, where regular

convolutions are replaced with depthwise separable convolutions and attention is added between residual connections.

Depthwise separable convolutions are widely used in the computer vision literature to replace regular convolutions, as they're empirically shown to perform comparably to regular convolutions with a fraction of the trainable parameters. Depthwise separable convolutions consist of two steps. The first step is the depthwise convolution that this MBConv also utilizes, and in the second step, a 1x1 convolution is applied to map input features into output features of the intended feature map size.

SmAt-UNet utilizes the Convolutional Block Attention Module (CBAM) (Woo et al., 2018). CBAM consists of two different types of attention, namely, channel attention and spatial attention. Channel attention uses a process that is quite similar to the squeeze and excitation modules with a few alterations, and the spatial attention module of CBAM obtains a 2D descriptor that denotes channel information at each pixel over all grid cells before constructing a 2D spatial attention map. The raw attention map is then obtained by applying a convolution layer to the 2D descriptor. The details of CBAM can be seen in Woo et al., 2018.

3.3. Baselines

Beside the aforementioned neural network architectures, we also utilize a few baselines that will be compared to EfficientRainNet in nowcasting twelve rainfall maps into the future over the IowaRain dataset.

3.3.1. Persistence

Persistence, or the nearest frame, could be defined by the "tomorrow is going to be the same as today" principle (Krajewski et al., 2021). In other words, persistence forecasts always use the latest known frame. Persistence calculations were done using a rainfall nowcasting package in Python that has many conventional extrapolation methods implemented, rainymotion (Ayzel et al., 2019).

3.3.2. Optical Flow

Optical flow is used in computer vision literature for a variety of purposes (Gao et al., 2010; Buades et al., 2016). The summary of the spatial changes in objects between two frames of a scene is called optical flow. In order to evaluate the mobility of velocity fields between two frames, optical flow demonstrates the motion of the objects. Consequently, an algorithm for figuring out how objects travel from one scene to another is an optical flow algorithm. The characteristics that each pixel in a scene possesses are known as its "pixel intensity" in computer vision, and what an optical flow algorithm does is calculate the change in pixel intensities. In a 2D plane, a pixel's intensity is determined by its position within that 2D plane and its value. Since rainfall maps are 2D tensors, the same phenomenon holds true for the instance we analyze in this work.

The computer vision literature has a wide variety of optical flow computation algorithms. In this study, we used the Gunnar-Farneback optical flow, also known as dense optical flow (Farneback, 2003). Gunnar-Farneback optical flow is called "dense" as opposed to "sparse" because it calculates pixel intensities for each and every pixel in the scene rather than feature-level intensity computations. This would entail computing the changes for each measurement along the regions that make up the 2D rain map. The mathematical formulation of the algorithm is outside the scope of this study; for more information, we advise the reader to check the referred study. In this study, we employ the Rainymotion library for advection correction using dense optical flow and refer to the method as "Optical Flow" throughout this manuscript.

3.3.3. High Resolution Rapid Refresh (HRRR)

HRRR is a real-time convection-allowing NWP model updated hourly and initialized by 3-km grids with radar assimilation (Dowell et al. 2022). HRRR is dependent on its parent models, radar-assimilating Rapid Refresh (RAP) and radar-enhanced Rapid Update Cycle (RUC). The HRRR model provides QPF for up to 18 hours (48 hours at every sixth hour) at 3-km and hourly resolutions, while it also creates experimental sub-hourly products. To show how EfficientRainNet performs in comparison to HRRR, this study will share a comparison table for HRRR. Since rainfall sequences typically do not start at full clock hours, only matching timestamps between the HRRR forecasts collected at the start of the hour and the test dataset we employed were used.

Since there is a temporal resolution mismatch between the proposed neural networks and HRRR (the temporal resolution of the neural networks we propose is 10 minutes as opposed to HRRR's one hour), only matching timestamps between the HRRR forecasts collected and the test dataset we employed were used. In other words, a forecast for a test dataset entry might start at 12.10 p.m., while HRRR doesn't have a forecast made at that hour, as it only has them for full hours. In order to circumvent this issue, we will only use test dataset entries that start at full hours (1.00 p.m., 2.00 p.m., etc.) when we report metrics in comparison to HRRR.

3.4. Training, Metrics and Evaluation

All the networks that were described above were implemented on the PyTorch numeric computing library (Paszke et al., 2019) and were trained using RMSProp as the optimizer and Mean Absolute Error (MAE) as the cost function on NVIDIA Titan V GPUs. Each of the approaches above will be compared using a variety of metrics, namely the Correlation Coefficient (R), Critical Success Index (CSI), Heidke Skill Score (HSS), Possibility of Detection (POD), False Alarm Rate (FAR), Accuracy, Precision, F-score, and Number of Trainable Parameters for two threshold values of 0.01 mm/hr and 0.5 mm/hr precipitation. The formulation of metrics can be seen in Table 2 and (1-9). It should be noted that while the best value for POD, CSI, HSS, Accuracy, Precision and F-score is 1.0 (the greater the better), it is 0.0 for FAR and MAE (the lower the better). The Correlation of Coefficient ranges between -1 and 1, with 1 being the best.

Table 2. Contingency table for metrics

		Real Values	
		Rain	No Rain
Predicted Values	Rain	TP	FP
	No Rain	FN	TN

$$MAE = \frac{\sum_{i=1}^n |prediction_i - observation_i|}{n} \quad (Eq. 1)$$

$$R_{ij} = \frac{C_{ij}}{\sqrt{C_{jj}C_{ii}}} \quad (Eq. 2)$$

$$CSI = \frac{TP}{TP + FN + FP} \quad (Eq. 3)$$

$$HSS = \frac{TP \times TN - FN \times FP}{(TP + FN) \times (FN + TN) + (TP + FP) \times (FP + TN)} \quad (Eq. 4)$$

$$POD = \frac{TP}{TP + FN} \quad (Eq. 5)$$

$$FAR = \frac{FP}{TP + FP} \quad (Eq. 6)$$

$$Accuracy = \frac{TN + TP}{TP + FP + TN + FN} \quad (Eq. 7)$$

$$Precision = \frac{TP}{TP + FP} \quad (Eq. 8)$$

$$F - score = \frac{TP}{TP + \frac{1}{2}(FP + FN)} \quad (Eq. 9)$$

4. Experiments and Dataset

In this section, the dataset that was employed throughout the study and the experiments will be described and detailed.

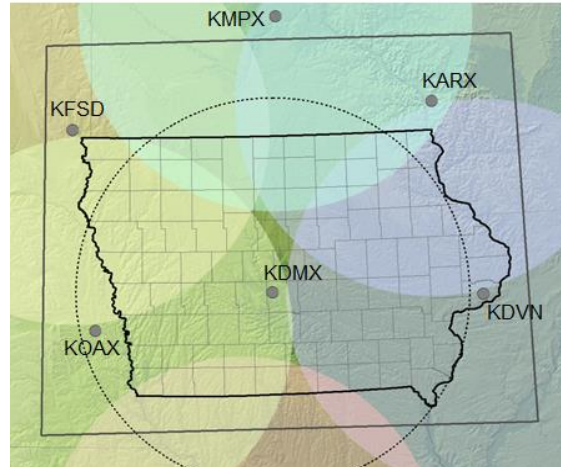


Figure 6. Next Generation Weather Radar (NEXRAD) system, which the IowaRain data source, radar coverage over the State of Iowa

4.1. IowaRain Dataset and Problem Definition

The IowaRain (Sit et al., 2021a) is a rainfall event benchmark dataset for the State of Iowa, designed to support streamflow forecasting studies (Xiang et al., 2021; Sit et al., 2021b). It is the dataset used throughout this study. The Iowa Flood Center's Quantitative Precipitation Estimation (QPE) system, which uses seven NEXRAD radars to cover the entire State of Iowa, is the primary source of the IowaRain dataset (Seo and Krajewski, 2020) (Figure 6). The information from IowaRain has temporal and spatial resolutions of five minutes and approximately 500 meters, respectively. 288 rainfall events from 2016 to 2019 are included in IowaRain. Each rainfall event is made up of a collection of 2D rain maps or images taken at five-minute intervals.

This study only uses rainfall maps for nowcasting, and for this purpose, it utilizes a temporally and spatially scaled subset of IowaRain that covers a large watershed in eastern Iowa (Figure 7). From the original IowaRain domain, a region that covers the Iowa River basin was selected, and then the temporal and spatial resolutions were changed to 10 minutes and 3 kilometers, respectively, from the original resolutions of 5 minutes and 500 meters. Consequently, for each rainfall map, the matrix dimension was reshaped to 128 x 128 from 1088 x 1760. This process was undertaken in order to decrease the input and output sizes to maintain viable memory and computation requirements and match HRRR's spatial resolution of 3 kilometers. At the end, the methods that are presented in this study will be given the input of twelve 128 x 128 rainfall maps to forecast twelve 128 x 128 rainfall maps into the future (Figure 8). The input-output length of 12 was chosen for a few reasons: (1) the state-of-the-art approaches typically are tested with the same length of input and output sequences (Shi et al., 2015; Shi et al., 2017); (2) we wanted to have at least 2 hours of forecasts as any smaller than 12 sequence length would only yield one comparable result to HRRR per dataset entry, and we wanted to investigate the change as lead time increases; and (3) nowcasting literature using deep

learning has typically proposed approaches to forecast up to 100 minutes (Trebing et al., 2021; Shi et al., 2017) and we wanted to present a comparable option by design.

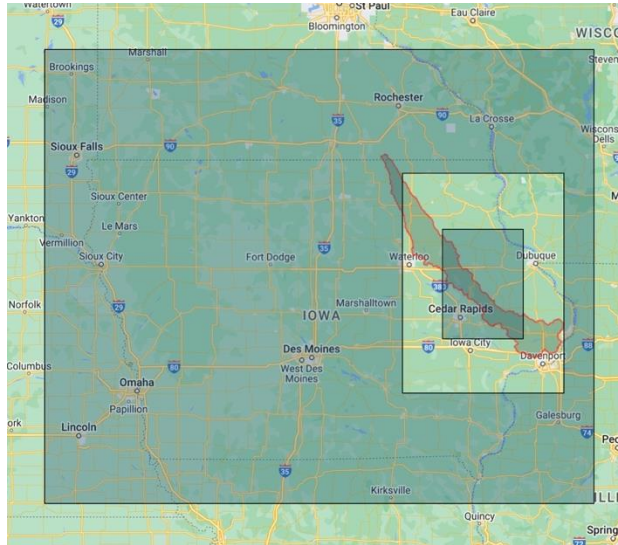


Figure 7. Whole IowaRain domain (big darker rectangle), IowaRain subset domain (small lighted rectangle) and centered test domain (smallest darker rectangle) along with the basin boundary over Google Maps

HRRR has been running forecasts for years, but during the time period of IowaRain, the most complete forecast data from HRRR in our records was 2017. Thus, we use rainfall events from 2017 as the testing set, while rainfall events from 2016, 2018, and 2019 are used as the training set. Even though all the methods in the previous section will be compared over the whole domain described above, since rainfall trajectory and density change drastically and rather quickly, the performances of the methods will also be reported for a central area that will be clipped from the whole region. This clipping results in a set of frames that are 64 x 64 as opposed to 128 x 128.

4.2. Sensitivity Studies

In order to understand how models' behavior changes in different experiment settings, we will present three ablation studies and share performance metrics for them:

With more and less input sizes - The main experiment in this study is to forecast 12 future frames using 12 past frames, but it is important to experiment with different input sizes and the impact of input size on various output sizes. For this reason, all the performance metrics will be shared for various input and output sizes ranging from 6 to 24.

Utilization of Fused MBConv - The building block this study employs is from EfficientNetV2. The EfficientNetV2 architecture also utilizes a mobile convolution block that is a variation of MBConv and is named Fused MBConv. In Fused MBConv, instead of the first two operations, where a 3x3 depthwise convolution is followed by a 1x1 convolution, a single 3x3 convolution is employed, and the SE Layer is discarded. Furthermore, in EfficientNetv2, authors

articulate that employing Fused MBConv in the first few layers instead of MBConv improves performance. To see if this claim holds true in the nowcasting case, a set of metrics will be provided for EfficientRainNet where the first few MBConv blocks are replaced with Fused MBConv.

Activation Function and Batch Normalization - The swish function is used by MBConv, but in experiments that shaped this study, we discovered that using LeakyReLU with a slope of 0.1 works better for a different direction, nowcasting over the IowaRain domain. To show this, we will also share the performance of EfficientRainNet, where the activation function is swish instead of LeakyReLU. Similarly, we will also explore the performance changes with batch normalization that we discarded for the sake of better performance.

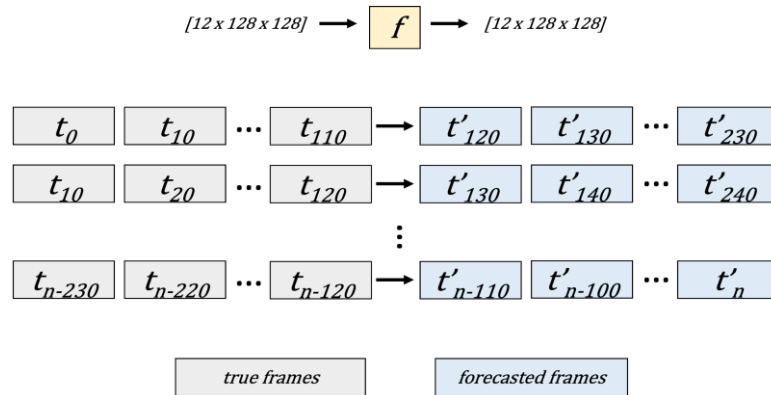


Figure 8. Input/Output data size and task summary

5. Results and Discussion

In this section, results of various tests using the methodology described in the previous section will be shared, starting with the main task this study investigates: forecasting 120 minutes of precipitation using 120 minutes of historic measurements with 10 minutes of temporal resolution. All the metrics given in this section were calculated using the entirety of the test dataset. Individually visualized forecasts of three rainfall events could be seen in Appendix Figures A1-A3.

Table 3. Performances of methodologies over 12 frames of forecasts for the whole region. The best score is highlighted in **bold**; the second best is underlined. >0.05 and >0.1 represents two threshold values in mm/hr.

Algorithms	MAE ▼	R ▲	CSI ▲		HSS ▲		POD ▲		FAR ▼		ACC ▲		Precision ▲		F-score ▲	
			>0.05	>0.1	>0.05	>0.1	>0.05	>0.1	>0.05	>0.1	>0.05	>0.1	>0.05	>0.1	>0.05	>0.1
Persistence	1.745	0.231	0.486	0.471	0.427	0.42	0.649	0.635	0.369	0.383	0.749	0.75	0.631	0.617	0.635	0.621
Dense OpticalFlow	1.361	0.423	0.617	0.605	0.614	0.609	0.764	0.752	<u>0.243</u>	<u>0.251</u>	0.832	0.833	<u>0.757</u>	<u>0.749</u>	0.755	0.745
ConvGRU	<u>0.947</u>	0.575	0.634	0.627	<u>0.625</u>	0.630	0.822	0.801	0.270	0.262	<u>0.833</u>	<u>0.839</u>	0.730	0.738	0.769	0.763
SmAt-UNet	1.026	0.506	0.588	0.584	0.558	0.570	<u>0.799</u>	<u>0.779</u>	0.314	0.304	0.792	0.805	0.686	0.696	0.728	0.726
EfficientRainNet	0.945	<u>0.529</u>	<u>0.628</u>	<u>0.617</u>	0.633	0.629	0.759	0.744	0.220	0.223	0.843	0.844	0.780	0.777	<u>0.763</u>	0.754

Table 3, where the best score is highlighted in bold and the second best is underlined, reports scores for various metrics for each of the described methodologies with two different rainfall threshold values in mm/hr where applicable. Even though Mean Absolute Error (MAE) is not an ideal metric for rainfall forecasts, since neural networks were trained using MAE as the cost function, it is still an important metric over the ability to learn for the neural networks presented here. As the presented MAE scores show, all neural networks are able to outperform the Persistence and Dense OpticalFlow baselines, while ConvGRU and EfficientRainNet perform preferably better than SmAt-UNet. Similar trends could be seen over forecast performance metrics and indices, such as CSI and HSS. While ConvGRU and EfficientRainNet provide comparable performances with trivial differences, SmAt-UNet could fall behind Optical Flow.

One important takeaway from the table is about POD and FAR. While in POD, ConvGRU is drastically better than EfficientRainNet, in FAR the order is quite different. This phenomenon could be explained by ConvGRU's proclivity to generate false positives, whereas EfficientRainNet has a higher threshold for forecasting rainfall. Precision and Recall follow this suit and thus affect how the F-Score is shaped. Although the performance differences between ConvGRU and EfficientRainNet are typically trivial, it should be noted that EfficientRainNet accomplishes this by using drastically fewer trainable parameters, making it faster to train and forecast. Following a similar fashion, Figures 9 and 10 show the same scores for all the approaches for individual forecasted frames. As one would expect, the performance deteriorates as forecast time increases. One thing that catches attention is the fact that, at the first forecasted frame, the optical flow-based method outperforms all other methods. EfficientRainNet mostly provides a comparable performance to ConvGRU over each of the forecasted frames and mostly outperforms ConvGRU over the first hour but is somewhat inferior over the second hour.

Tables 4 and 5 show the performances of all the methodologies described in the methodology section for the first hour of forecasts and the second hour of forecasts, respectively. In Tables 4 and 5, performances are in accordance with individual frame scores, as during the first hour, the best scores are distributed between Optical Flow and EfficientRainNet, but over the second hour, ConvGRU gets better.

Table 4. Performances of methodologies over first hour of forecasts, or average of first 6 frames, of total 12 forecasted frames. The best score is highlighted in **bold**; the second best is underlined.

Algorithms	MAE ▼	R▲	CSI ▲		HSS ▲		POD ▲		FAR ▼		ACC ▲		Precision ▲		F-score ▲	
			>0.05	>0.1	>0.05	>0.1	>0.05	>0.1	>0.05	>0.1	>0.05	>0.1	>0.05	>0.1	>0.05	>0.1
Persistence	1.397	0.444	0.632	0.620	0.586	0.585	0.670	0.666	0.096	0.114	0.802	0.805	0.904	0.886	0.764	0.754
Dense OpticalFlow	0.792	0.746	0.816	0.804	0.784	0.784	0.886	0.879	0.091	0.098	0.900	0.900	0.909	0.902	0.896	0.889
ConvGRU	0.669	0.726	0.804	0.793	0.777	0.780	<u>0.862</u>	<u>0.846</u>	0.077	0.074	0.896	0.897	0.923	0.926	0.889	0.882
SmAt-UNet	0.735	<u>0.775</u>	0.759	0.761	0.704	0.725	0.857	0.853	0.128	0.122	0.855	0.866	0.872	0.878	0.856	0.858
EfficientRainNet	0.658	0.790	0.794	0.782	<u>0.773</u>	0.773	0.829	0.817	0.051	0.053	0.894	0.894	0.949	0.947	0.882	0.874

Table 5. Performances of methodologies over second hour of forecasts, or average of second 6 frames, of total 12 forecasted frames. The best score is highlighted in **bold**; the second best is underlined.

Algorithms	MAE ▼	R ▲	CSI ▲		HSS ▲		POD ▲		FAR ▼		ACC ▲		Precision ▲		F-score ▲	
			>0.05	>0.1	>0.05	>0.1	>0.05	>0.1	>0.05	>0.1	>0.05	>0.1	>0.05	>0.1	>0.05	>0.1
Persistence	1.837	0.158	0.466	0.446	0.334	0.325	0.560	0.547	0.295	0.323	0.681	0.682	0.705	0.677	0.613	0.593
Dense OpticalFlow	1.303	0.416	0.647	0.627	0.566	0.561	0.767	0.753	0.195	0.211	0.798	0.797	0.805	0.789	0.777	0.761
ConvGRU	0.912	0.606	0.644	0.621	0.584	0.580	0.742	0.714	0.168	0.172	0.803	0.804	0.832	0.828	0.773	0.754
SmAt-UNet	0.955	0.457	0.606	0.586	0.524	0.528	0.723	0.692	0.205	0.203	0.770	0.774	0.795	0.797	0.746	0.729
EfficientRainNet	0.927	0.457	0.610	0.586	0.561	0.553	0.675	0.652	0.136	0.144	0.793	0.793	0.864	0.856	0.742	0.722

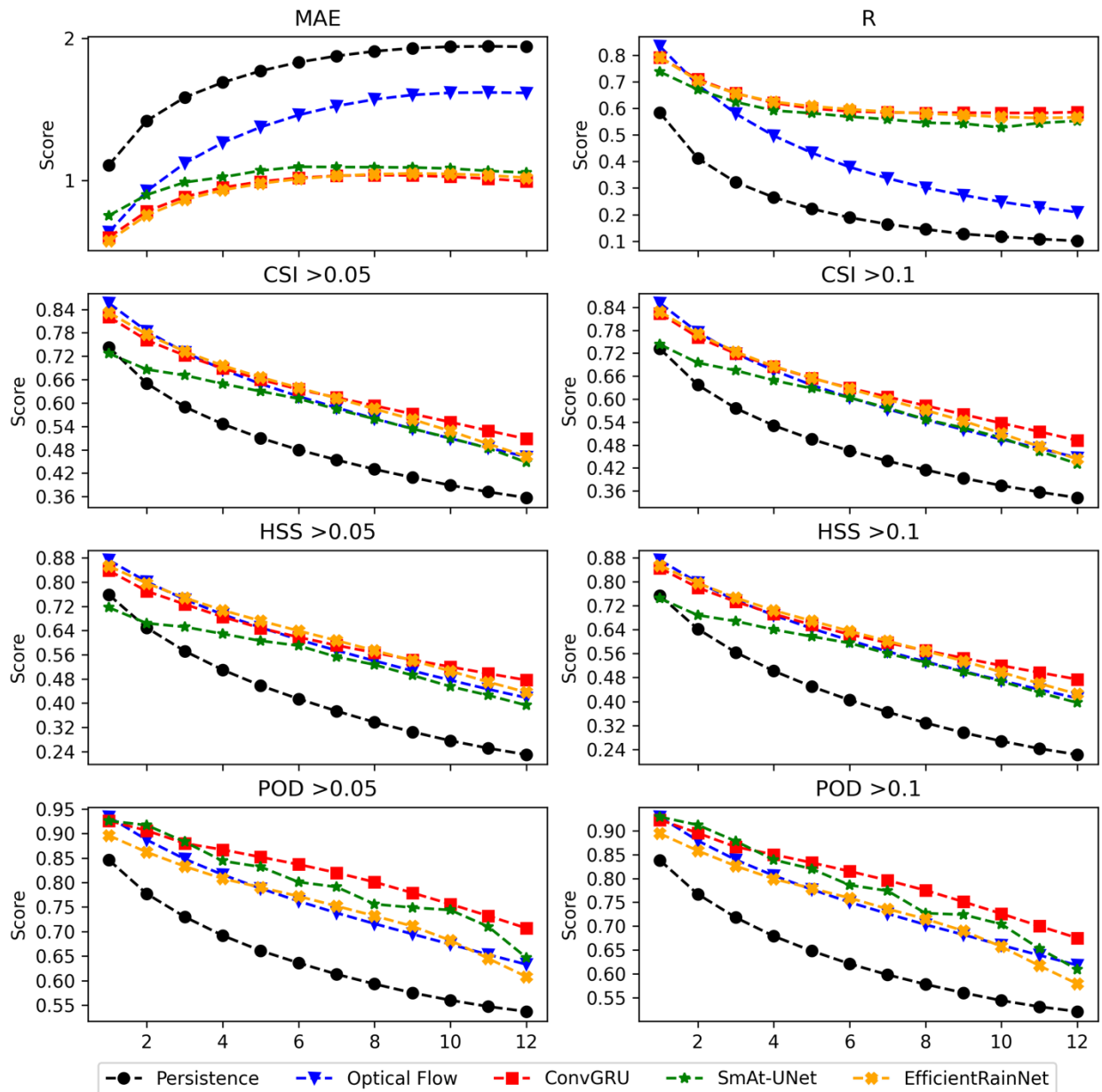


Figure 8. Score changes for MAE, R, CSI, HSS and POD over the forecasted frames for two thresholds wherever applicable

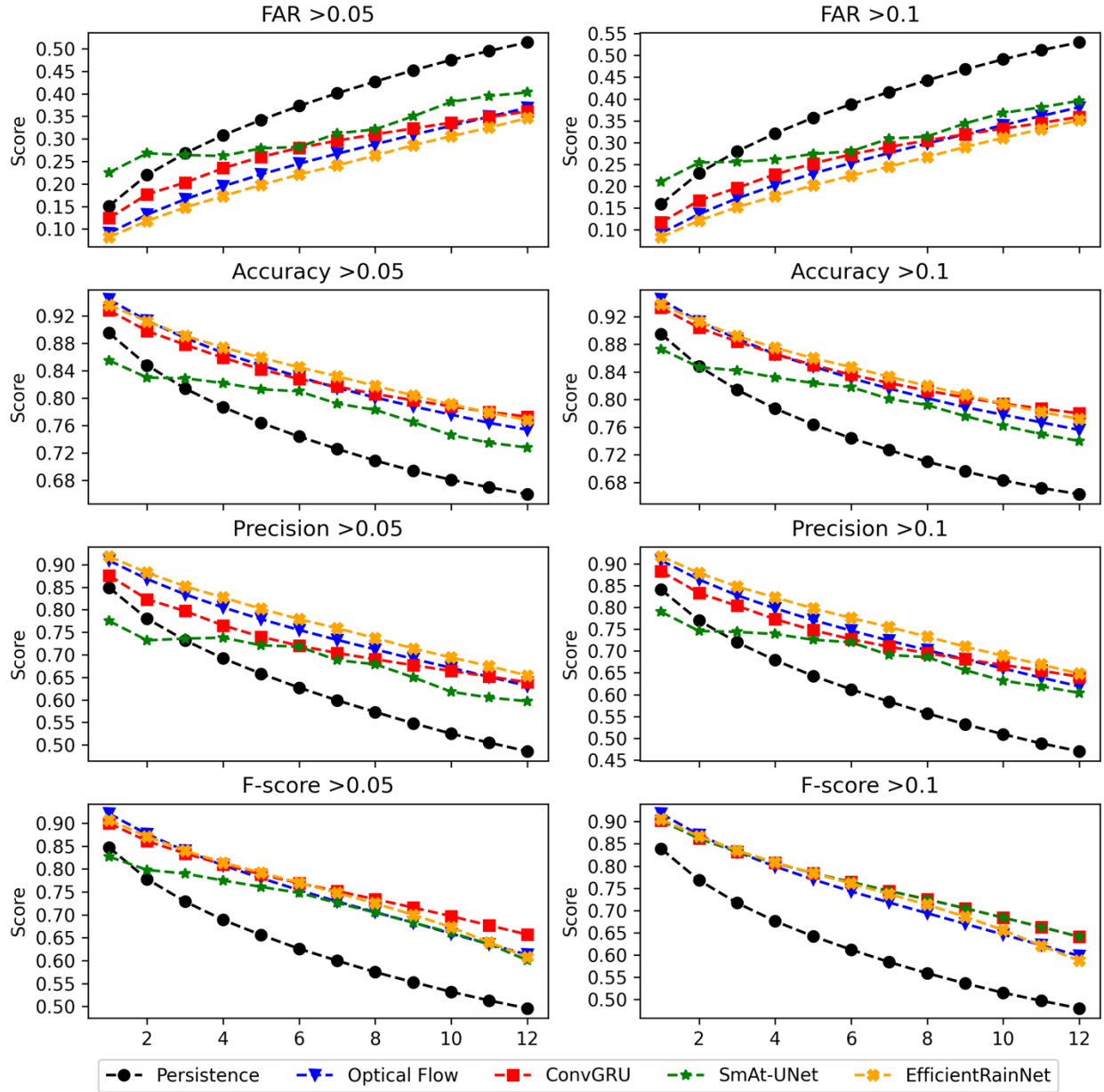


Figure 9. Score changes for FAR, Accuracy, Precision, F-score over the forecasted frames for two thresholds wherever applicable

Table 6. Performances of methodologies over 12 frames of forecasts for centered region. The best score is highlighted in **bold**; the second best is underlined.

Algorithms	MAE ▼	R▲	CSI ▲		HSS ▲		POD ▲		FAR ▼		ACC ▲		Precision ▲		F-score ▲	
			>0.05	>0.1	>0.05	>0.1	>0.05	>0.1	>0.05	>0.1	>0.05	>0.1	>0.05	>0.1		
Persistence	2.380	0.190	0.440	0.426	0.287	0.283	0.631	0.617	0.406	0.419	0.703	0.703	0.594	0.581	0.587	0.573
Dense OpticalFlow	1.610	0.426	0.595	0.582	0.539	0.536	0.744	0.731	<u>0.259</u>	<u>0.266</u>	<u>0.824</u>	<u>0.824</u>	<u>0.741</u>	<u>0.734</u>	0.732	0.723
ConvGRU	1.194	0.530	0.610	0.603	0.532	0.543	0.827	0.803	0.304	0.295	0.817	<u>0.824</u>	0.696	0.705	0.744	0.739
SmAt-UNet	1.284	0.503	0.563	0.559	0.455	0.475	<u>0.816</u>	<u>0.794</u>	0.359	0.349	0.768	0.782	0.641	0.651	0.701	0.699
EfficientRainNet	<u>1.199</u>	<u>0.524</u>	<u>0.599</u>	<u>0.588</u>	<u>0.537</u>	<u>0.538</u>	0.743	0.727	0.248	0.248	0.826	0.827	0.752	0.752	<u>0.733</u>	<u>0.724</u>

Since rain moves over a vast 2D region rather quickly, it is important to run an experiment to see how precipitation forecast methods perform over a centered area within the whole study domain. For this very reason, a subarea within the defined domain of this study was clipped. This centered region's data has 3 km of spatial resolution and 10 minutes of temporal resolution, but only one-fourth of the total area with a size of 64x64, down from 128x128. The same metrics over the centered area for all of the methodologies could be found in Table 6. Scores in Table 6 are, for the most part, in accordance with whole-area performances. One major difference is that the optical flow-based approach seems to be more competitive in centered area forecasting than full area forecasting. SmAt-UNet follows suit and provides a comparable option, whereas leading scores are shared between ConvGRU and EfficientRainNet, again with drastically fewer trainable parameters.

Table 7. Performances of variations of EfficientRainNet over the forecasted 12 frames. The best score is highlighted in **bold**; the second best is underlined.

Algorithms	MAE ▼	R▲	CSI ▲		HSS ▲		POD ▲		FAR ▼		ACC ▲		Precision ▲		F-score ▲	
			>0.05	>0.1	>0.05	>0.1	>0.05	>0.1	>0.05	>0.1	>0.05	>0.1	>0.05	>0.1	>0.05	>0.1
w/ BN	1.027	0.508	0.594	0.588	0.597	0.597	0.718	0.718	0.225	0.236	0.822	0.825	0.775	0.764	0.738	0.733
w/ Sw	0.945	<u>0.532</u>	0.632	0.625	0.620	0.629	<u>0.825</u>	<u>0.786</u>	0.275	0.252	0.831	0.841	0.725	0.748	0.767	0.760
w/ BN + Sw	<u>0.947</u>	0.533	0.625	0.625	0.601	0.621	0.859	0.818	0.308	0.279	0.817	0.834	0.692	0.721	0.761	0.760
w/ TempNet	0.948	0.524	<u>0.629</u>	0.615	0.633	<u>0.628</u>	0.758	0.738	<u>0.220</u>	<u>0.220</u>	0.843	0.845	<u>0.780</u>	<u>0.780</u>	<u>0.763</u>	0.752
w/ Fused MBConv	0.950	0.525	0.621	0.609	<u>0.626</u>	0.622	0.744	0.728	0.217	0.219	<u>0.840</u>	0.842	0.783	0.781	0.758	0.747
EfficientRainNet	0.945	0.529	0.628	<u>0.617</u>	0.633	0.629	0.759	0.744	<u>0.220</u>	0.223	0.843	<u>0.844</u>	<u>0.780</u>	<u>0.777</u>	<u>0.763</u>	<u>0.754</u>

Table 7, which shows sensitivity performances, suggests that when LeakyReLU is replaced with the swish function, the metrics on which EfficientRainNet focuses change. Even though the metric they were trained on is the same, EfficientRainNet with LeakyReLU tends to provide better HSS and FAR scores, whereas with the swish function, it becomes more competitive over CSI and POD, which appear to be ConvGRU's strong suits. Scores show that EfficientRainNet with FusedMBConv for the first few MBConv layers instead performs worse than the original EfficientRainNet overall, and it comes with additional trainable parameters. Thus, we were not able to observe the performance gain that was shown in EfficientNet-v2. Furthermore, in Table 8, we show various input/output length pairs and MAE performance for EfficientRainNet. As the scores in the table suggest, as the input length increases, the performance also improves. One other suggestion is that an input length of 2 already, most of the time, gives comparable performance to SmAt-UNet.

HRRR data that was available to us had hourly resolution and was only saved at full clocks. Thus, comparisons with HRRR follow a different workflow. Over our test dataset datetime range, which is the year 2017, we first found the intersection of HRRR and our test dataset, which was to take every dataset entry where the forecast hour was a full clock. Then, among those, we aggregated the observations with the temporal resolution of five minutes, which is the original temporal resolution of IowaRain, to get as close to the ground truth as possible because HRRR is modeled over higher temporal resolutions than the 10-minutes that we employ in this

study. At the end, comparisons were made with each model’s forecasts averaged into hourly frames by averaging (t0, t1, ..., t6, total of 7 frames for the first hour, and t6, t7, ... t12, for a total of 7 frames for the second hour). Tables 9 and 10 show how each of the methodologies in this paper compares to HRRR.

Table 8. Input/Output length pairs and their performance over MAE for EfficientRainNet

Input Length	Output Length			
	12	16	20	24
2	0.986	1.048	1.088	1.111
4	0.987	1.047	1.085	1.105
6	0.980	1.037	1.077	1.097
8	0.973	1.032	1.064	1.088
10	0.959	1.019	1.055	1.079
12	0.945	1.009	1.042	1.064

Although the evaluation data is somewhat limited, these results indicate that, for the most part, deep learning models provide viable alternatives to HRRR, particularly when compared to the metric that they were trained on. However, for the first two hours, Optical flow was still mostly better than HRRR, which again shows HRRR is not the way to go for nowcasting.

Table 9. Performances of each methodology and HRRR for the first hour over the available HRRR forecast data. The best score is highlighted in **bold**; the second best is underlined.

Algorithms	MAE ▼	R ▲	CSI ▲		HSS ▲		POD ▲		FAR ▼		ACC ▲		Precision ▲		F-score ▲	
			>0.05	>0.1	>0.05	>0.1	>0.05	>0.1	>0.05	>0.1	>0.05	>0.1	>0.05	>0.1	>0.05	>0.1
Persistence	1.102	0.619	0.683	0.672	0.660	0.661	0.704	0.704	0.046	<u>0.068</u>	0.837	0.841	0.954	0.932	0.804	0.796
Dense OpticalFlow	0.685	0.768	0.812	0.799	0.783	0.783	<u>0.881</u>	0.875	0.090	<u>0.101</u>	0.899	0.899	0.910	0.899	0.895	0.886
HRRR	1.555	0.446	0.709	0.693	0.587	0.608	0.908	<u>0.872</u>	0.232	0.226	0.810	0.815	0.768	0.774	0.825	0.813
ConvGRU	0.554	0.828	0.796	0.788	0.770	0.778	0.854	<u>0.842</u>	0.080	0.077	<u>0.892</u>	<u>0.896</u>	<u>0.920</u>	<u>0.923</u>	0.884	0.878
SmAt-UNet	0.639	0.815	0.762	0.765	0.719	0.742	0.853	0.855	0.122	0.121	0.864	0.876	0.878	0.879	0.859	0.861
Persistence	0.541	0.832	0.783	0.775	0.764	0.770	0.816	0.810	<u>0.050</u>	0.054	0.889	0.894	0.950	0.946	0.875	0.870

Table 10. Performances of each methodology and HRRR for the second hour over the available HRRR forecast data. The best score is highlighted in **bold**; the second best is underlined.

Algorithms	MAE ▼	R ▲	CSI ▲		HSS ▲		POD ▲		FAR ▼		ACC ▲		Precision ▲		F-score ▲	
			>0.05	>0.1	>0.05	>0.1	>0.05	>0.1	>0.05	>0.1	>0.05	>0.1	>0.05	>0.1	>0.05	>0.1
Persistence	1.723	0.208	0.479	0.459	0.354	0.346	0.559	0.546	0.267	0.299	0.687	0.690	0.733	0.701	0.625	0.605
Dense OpticalFlow	1.177	0.432	0.652	0.627	<u>0.577</u>	<u>0.570</u>	<u>0.755</u>	<u>0.738</u>	0.171	0.191	0.802	0.800	0.829	0.809	0.783	0.764
HRRR	1.763	0.284	0.598	0.568	0.425	0.433	0.817	0.772	0.303	0.312	0.733	0.732	0.697	0.688	0.741	0.716
ConvGRU	0.883	0.548	<u>0.647</u>	<u>0.626</u>	0.588	0.588	0.738	0.712	<u>0.156</u>	<u>0.159</u>	0.804	0.807	<u>0.844</u>	<u>0.841</u>	0.778	0.760
SmAt-UNet	0.923	0.486	0.614	0.594	0.542	0.548	0.713	0.686	0.180	0.181	0.778	0.784	0.820	0.819	0.753	0.737
Persistence	<u>0.884</u>	<u>0.522</u>	0.612	0.590	0.569	0.565	0.668	0.648	0.111	0.120	0.796	0.798	0.889	0.880	0.748	0.729

6. Conclusion

In this study, a memory-wise efficient neural network architecture, namely EfficientRainNet, that is based on mobile inverted residual linear bottleneck blocks for rainfall nowcasting was

presented. The performance of the proposed EfficientRainNet was compared to two baselines: persistence and dense optical flow-based advection correction, and two neural network architectures from the nowcasting literature. These two NN architectures are encoder-decoder ConvGRUs, which is widely used as a reference point for nowcasting approaches, and Small Attention UNet (SmAt-UNet), which is another memory efficiency-focused neural network architecture for rainfall nowcasting. The presented results have shown that EfficientRainNet, for the most part, outperforms SmAt-UNet and provides comparable results to ConvGRUs, with less than 6% of trainable parameters in ConvGRU and less than 9% of trainable parameters in SmAt-UNet.

Potential improvement for the current study could be to train and validate the EfficientRainNet over wider regions with higher temporal and spatial resolutions as well as for increased forecast ranges with more data points along with historical precipitation values. As EfficientRainNet is small enough to run on mobile devices, another outlook for this study is to test the practicality of EfficientRainNet on edge devices for more practical climate modeling in not only a limited area but for vast regions all around the globe.

References

- Alabbad, Y. and Demir, I., 2022. Comprehensive flood vulnerability analysis in urban communities: Iowa case study. *International journal of disaster risk reduction*, 74, p.102955.
- Alabbad, Y., Yildirim, E. and Demir, I., 2022. Flood mitigation data analytics and decision support framework: Iowa Middle Cedar Watershed case study. *Science of The Total Environment*, 814, p.152768.
- Aly, M.M.S., Gao, M., Hills, G., Lee, C.S., Pitner, G., Shulaker, M.M., Wu, T.F., Asheghi, M., Bokor, J., Franchetti, F. and Goodson, K.E., 2015. Energy-efficient abundant-data computing: The N3XT 1,000 x. *Computer*, 48(12), pp.24-33.
- Ayzel, G., Heistermann, M. and Winterrath, T., 2019. Optical flow models as an open benchmark for radar-based precipitation nowcasting (rainymotion v0. 1). *Geoscientific Model Development*, 12(4), pp.1387-1402.
- Ayzel, G., Scheffer, T. and Heistermann, M., 2020. RainNet v1. 0: a convolutional neural network for radar-based precipitation nowcasting. *Geoscientific Model Development*, 13(6), pp.2631-2644.
- Badrinarayanan, V., Kendall, A. and Cipolla, R., 2017. Segnet: A deep convolutional encoder-decoder architecture for image segmentation. *IEEE transactions on pattern analysis and machine intelligence*, 39(12), pp.2481-2495.
- Buades, A., Lisani, J.L. and Miladinović, M., 2016. Patch-based video denoising with optical flow estimation. *IEEE Transactions on Image Processing*, 25(6), pp.2573-2586.
- Cao, Y., Li, Q., Shan, H., Huang, Z., Chen, L., Ma, L. and Zhang, J., 2019. Precipitation nowcasting with star-bridge networks. *arXiv preprint arXiv:1907.08069*.

- Castro, R., Souto, Y.M., Ogasawara, E., Porto, F. and Bezerra, E., 2021. Stconvs2s: Spatiotemporal convolutional sequence to sequence network for weather forecasting. *Neurocomputing*, 426, pp.285-298.
- Chen, Y.H., Emer, J. and Sze, V., 2016. Eyeriss: A spatial architecture for energy-efficient dataflow for convolutional neural networks. *ACM SIGARCH Computer Architecture News*, 44(3), pp.367-379.
- Chin, T.W., Ding, R., Zhang, C. and Marculescu, D., 2020. Towards efficient model compression via learned global ranking. In *Proceedings of the IEEE/CVF conference on computer vision and pattern recognition* (pp. 1518-1528).
- Cools, J., Innocenti, D. and O'Brien, S., 2016. Lessons from flood early warning systems. *Environmental science & policy*, 58, pp.117-122.
- Davenport, F.V., Burke, M. and Diffenbaugh, N.S., 2021. Contribution of historical precipitation change to US flood damages. *Proceedings of the National Academy of Sciences*, 118(4).
- Demiray, B.Z., Sit, M. and Demir, I., 2021. DEM Super-Resolution with EfficientNetV2. *arXiv preprint arXiv:2109.09661*.
- Ding, R., Liu, Z., Blanton, R.D. and Marculescu, D., 2018. Lightening the load with highly accurate storage-and energy-efficient lightnns. *ACM Transactions on Reconfigurable Technology and Systems (TRETS)*, 11(3), pp.1-24.
- Dowell, D.C., Alexander, C.R., James, E.P., Weygandt, S.S., Benjamin, S.G., Manikin, G.S., Blake, B.T., Brown, J.M., Olson, J.B., Hu, M. and Smirnova, T.G., 2022. The High-Resolution Rapid Refresh (HRRR): An hourly updating convection-allowing forecast model. Part I: Motivation and system description. *Weather and Forecasting*, 37(8), pp.1371-1395.
- Espeholt, L., Agrawal, S., Sønderby, C., Kumar, M., Heek, J., Bromberg, C., Gazean, C., Hickey, J., Bell, A. and Kalchbrenner, N., 2021. Skillful twelve hour precipitation forecasts using large context neural networks. *arXiv preprint arXiv:2111.07470*.
- Ewing, G. and Demir, I., 2021. An ethical decision-making framework with serious gaming: a smart water case study on flooding. *Journal of Hydroinformatics*, 23(3), pp.466-482.
- Gao, P., Sun, X. and Wang, W., 2010, April. Moving object detection based on kirsch operator combined with Optical Flow. In *2010 International Conference on Image Analysis and Signal Processing* (pp. 620-624). IEEE.
- Gautam, A., Sit, M. and Demir, I., 2022. Realistic river image synthesis using deep generative adversarial networks. *Frontiers in water*, 4, p.10.
- Han, S., Liu, X., Mao, H., Pu, J., Pedram, A., Horowitz, M.A. and Dally, W.J., 2016. EIE: Efficient inference engine on compressed deep neural network. *ACM SIGARCH Computer Architecture News*, 44(3), pp.243-254.
- Han, S., Mao, H. and Dally, W.J., 2015. Deep compression: Compressing deep neural networks with pruning, trained quantization and huffman coding. *arXiv preprint arXiv:1510.00149*.
- He, K., Zhang, X., Ren, S. and Sun, J., 2016. Deep residual learning for image recognition. In *Proceedings of the IEEE conference on computer vision and pattern recognition* (pp. 770-778).

- Hering, A.M., Morel, C., Galli, G., Sényesi, S., Ambrosetti, P. and Boscacci, M., 2004, September. Nowcasting thunderstorms in the Alpine region using a radar based adaptive thresholding scheme. In Proceedings of ERAD (Vol. 1, No. 6).
- Hu, A. and Demir, I., 2021. Real-time flood mapping on client-side web systems using hand model. *Hydrology*, 8(2), p.65.
- Hu, J., Shen, L. and Sun, G., 2018. Squeeze-and-excitation networks. In Proceedings of the IEEE conference on computer vision and pattern recognition (pp. 7132-7141).
- Huang, J., Niu, D., Zang, Z., Chen, X. and Pan, X., 2021, October. RainfallNet: A Dual-Source of Spatial-Channel Attention Fusion Network for Precipitation Nowcasting. In *Journal of Physics: Conference Series* (Vol. 2050, No. 1, p. 012008). IOP Publishing.
- Inci, A., 2022. Scalable and Efficient Systems for Deep Learning, PhD thesis, Carnegie Mellon University, Pittsburgh, United States.
- Inci, A., Isgenc, M.M. and Marculescu, D., 2022a. Efficient Deep Learning Using Non-Volatile Memory Technology. arXiv preprint arXiv:2206.13601.
- Inci, A., Virupaksha, S.G., Jain, A., Chin, T.W., Thallam, V.V., Ding, R. and Marculescu, D., 2022b. QUIDAM: A Framework for Quantization-Aware DNN Accelerator and Model Co-Exploration. *ACM Transactions on Embedded Computing Systems (TECS)*.
- Jing, J., Li, Q. and Peng, X., 2019. MLC-LSTM: Exploiting the spatiotemporal correlation between multi-level weather radar echoes for echo sequence extrapolation. *Sensors*, 19(18), p.3988.
- Klocek, S., Dong, H., Dixon, M., Kanengoni, P., Kazmi, N., Lufarenko, P., Lv, Z., Sharma, S., Weyn, J. and Xiang, S., 2021. MS-nowcasting: Operational Precipitation Nowcasting with Convolutional LSTMs at Microsoft Weather. arXiv preprint arXiv:2111.09954.
- Krajewski, W.F., Ghimire, G.R., Demir, I. and Mantilla, R., 2021. Real-time streamflow forecasting: AI vs. Hydrologic insights. *Journal of Hydrology X*, 13, p.100110.
- Li, Z., Mount, J. and Demir, I., 2022. Accounting for uncertainty in real-time flood inundation mapping using HAND model: Iowa case study. *Natural Hazards*, 112(1), pp.977-1004.
- Luo, C., Li, X. and Ye, Y., 2020. PFST-LSTM: A spatiotemporal LSTM model with pseudoflow prediction for precipitation nowcasting. *IEEE Journal of Selected Topics in Applied Earth Observations and Remote Sensing*, 14, pp.843-857.
- Luo, C., Li, X., Wen, Y., Ye, Y. and Zhang, X., 2021. A novel LSTM model with interaction dual attention for radar echo extrapolation. *Remote Sensing*, 13(2), p.164.
- Luo, C., Ye, R., Li, X. and Ye, Y., 2021. RAP-Net: Region Attention Predictive Network for Precipitation Nowcasting. arXiv preprint arXiv:2110.01035.
- Montz, B.E. and Grunfest, E., 2002. Flash flood mitigation: recommendations for research and applications. *Global Environmental Change Part B: Environmental Hazards*, 4(1), pp.15-22.
- Paszke, A., Gross, S., Massa, F., Lerer, A., Bradbury, J., Chanan, G., Killeen, T., Lin, Z., Gimelshein, N., Antiga, L. and Desmaison, A., 2019. Pytorch: An imperative style, high-performance deep learning library. *Advances in neural information processing systems*, 32.

- Ronneberger, O., Fischer, P. and Brox, T., 2015, October. U-net: Convolutional networks for biomedical image segmentation. In International Conference on Medical image computing and computer-assisted intervention (pp. 234-241). Springer, Cham.
- Sandler, M., Howard, A., Zhu, M., Zhmoginov, A. and Chen, L.C., 2018. Mobilenetv2: Inverted residuals and linear bottlenecks. In Proceedings of the IEEE conference on computer vision and pattern recognition (pp. 4510-4520).
- Seo, B.C. and Krajewski, W.F., 2020. Statewide real-time quantitative precipitation estimation using weather radar and NWP model analysis: Algorithm description and product evaluation. *Environmental Modelling & Software*, 132, p.104791.
- Seo, B.C., Keem, M., Hammond, R., Demir, I. and Krajewski, W.F., 2019. A pilot infrastructure for searching rainfall metadata and generating rainfall product using the big data of NEXRAD. *Environmental modelling & software*, 117, pp.69-75.
- Shi, E., Li, Q., Gu, D. and Zhao, Z., 2018, February. A method of weather radar echo extrapolation based on convolutional neural networks. In International Conference on Multimedia Modeling (pp. 16-28). Springer, Cham.
- Shi, X., Chen, Z., Wang, H., Yeung, D.Y., Wong, W.K. and Woo, W.C., 2015. Convolutional LSTM network: A machine learning approach for precipitation nowcasting. *Advances in neural information processing systems*, 28.
- Shi, X., Gao, Z., Lausen, L., Wang, H., Yeung, D.Y., Wong, W.K. and Woo, W.C., 2017. Deep learning for precipitation nowcasting: A benchmark and a new model. *Advances in neural information processing systems*, 30.
- Sit, M., Demiray, B.Z., Xiang, Z., Ewing, G.J., Sermet, Y. and Demir, I., 2020. A comprehensive review of deep learning applications in hydrology and water resources. *Water Science and Technology*, 82(12), pp.2635-2670.
- Sit, M., Seo, B.C. and Demir, I., 2021a. Iowarain: A statewide rain event dataset based on weather radars and quantitative precipitation estimation. *arXiv preprint arXiv:2107.03432*.
- Sit, M., Demiray, B. and Demir, I., 2021b. Short-term hourly streamflow prediction with graph convolutional gru networks. *arXiv preprint arXiv:2107.07039*.
- Sønderby, C.K., Espeholt, L., Heek, J., Dehghani, M., Oliver, A., Salimans, T., Agrawal, S., Hickey, J. and Kalchbrenner, N., 2020. Metnet: A neural weather model for precipitation forecasting. *arXiv preprint arXiv:2003.12140*.
- Tan, M. and Le, Q., 2021, July. Efficientnetv2: Smaller models and faster training. In International Conference on Machine Learning (pp. 10096-10106). PMLR.
- Tang, Q., Yang, M. and Yang, Y., 2019. ST-LSTM: A deep learning approach combined spatio-temporal features for short-term forecast in rail transit. *Journal of Advanced Transportation*, 2019.
- Teague, A., Sermet, Y., Demir, I. and Muste, M., 2021. A collaborative serious game for water resources planning and hazard mitigation. *International Journal of Disaster Risk Reduction*, 53, p.101977.

- Trebing, K., Stańczyk, T. and Mehrkanoon, S., 2021. SmaAt-UNet: Precipitation nowcasting using a small attention-UNet architecture. *Pattern Recognition Letters*, 145, pp.178-186.
- Wang, Y., Gao, Z., Long, M., Wang, J. and Philip, S.Y., 2018, July. Predrnn++: Towards a resolution of the deep-in-time dilemma in spatiotemporal predictive learning. In *International Conference on Machine Learning* (pp. 5123-5132). PMLR.
- Wang, Y., Long, M., Wang, J., Gao, Z. and Yu, P.S., 2017. Predrnn: Recurrent neural networks for predictive learning using spatiotemporal lstms. *Advances in neural information processing systems*, 30.
- Werner, M. and Cranston, M., 2009. Understanding the value of radar rainfall nowcasts in flood forecasting and warning in flashy catchments. *Meteorological Applications: A journal of forecasting, practical applications, training techniques and modelling*, 16(1), pp.41-55.
- Woo, S., Park, J., Lee, J.Y. and Kweon, I.S., 2018. Cbam: Convolutional block attention module. In *Proceedings of the European conference on computer vision (ECCV)* (pp. 3-19).
- Xie, P., Li, X., Ji, X., Chen, X., Chen, Y., Liu, J. and Ye, Y., 2020. An energy-based generative adversarial forecaster for radar echo map extrapolation. *IEEE Geoscience and Remote Sensing Letters*.
- Xiang, Z., Demir, I., Mantilla, R. and Krajewski, W.F., 2021. A regional semi-distributed streamflow model using deep learning. *EarthArxiv*, 2152. <https://doi.org/10.31223/X5GW3V>
- Xiang, Z. and Demir, I., 2022. Real-Time Streamflow Forecasting Framework, Implementation and Post-Analysis Using Deep Learning. *EarthArxiv*, 3162. <https://doi.org/10.31223/X5BW6R>
- Xu, H., Muste, M. and Demir, I., 2019. Web-based geospatial platform for the analysis and forecasting of sedimentation at culverts. *Journal of Hydroinformatics*, 21(6), pp.1064-1081.
- Yan, B.Y., Yang, C., Chen, F., Takeda, K. and Wang, C., 2021. FDNet: A deep learning approach with two parallel cross encoding pathways for precipitation nowcasting. *arXiv preprint arXiv:2105.02585*.
- Yildirim, E. and Demir, I., 2022. Agricultural flood vulnerability assessment and risk quantification in Iowa. *Science of The Total Environment*, 826, p.154165.
- Yildirim, E., Just, C. and Demir, I., 2022. Flood risk assessment and quantification at the community and property level in the State of Iowa. *International Journal of Disaster Risk Reduction*, 77, p.103106.
- Zhong, S., Zeng, X., Ling, Q., Wen, Q., Meng, W. and Feng, Y., 2020, November. Spatiotemporal Convolutional LSTM for Radar Echo Extrapolation. In *2020 54th Asilomar Conference on Signals, Systems, and Computers* (pp. 58-62). IEEE.

Appendix

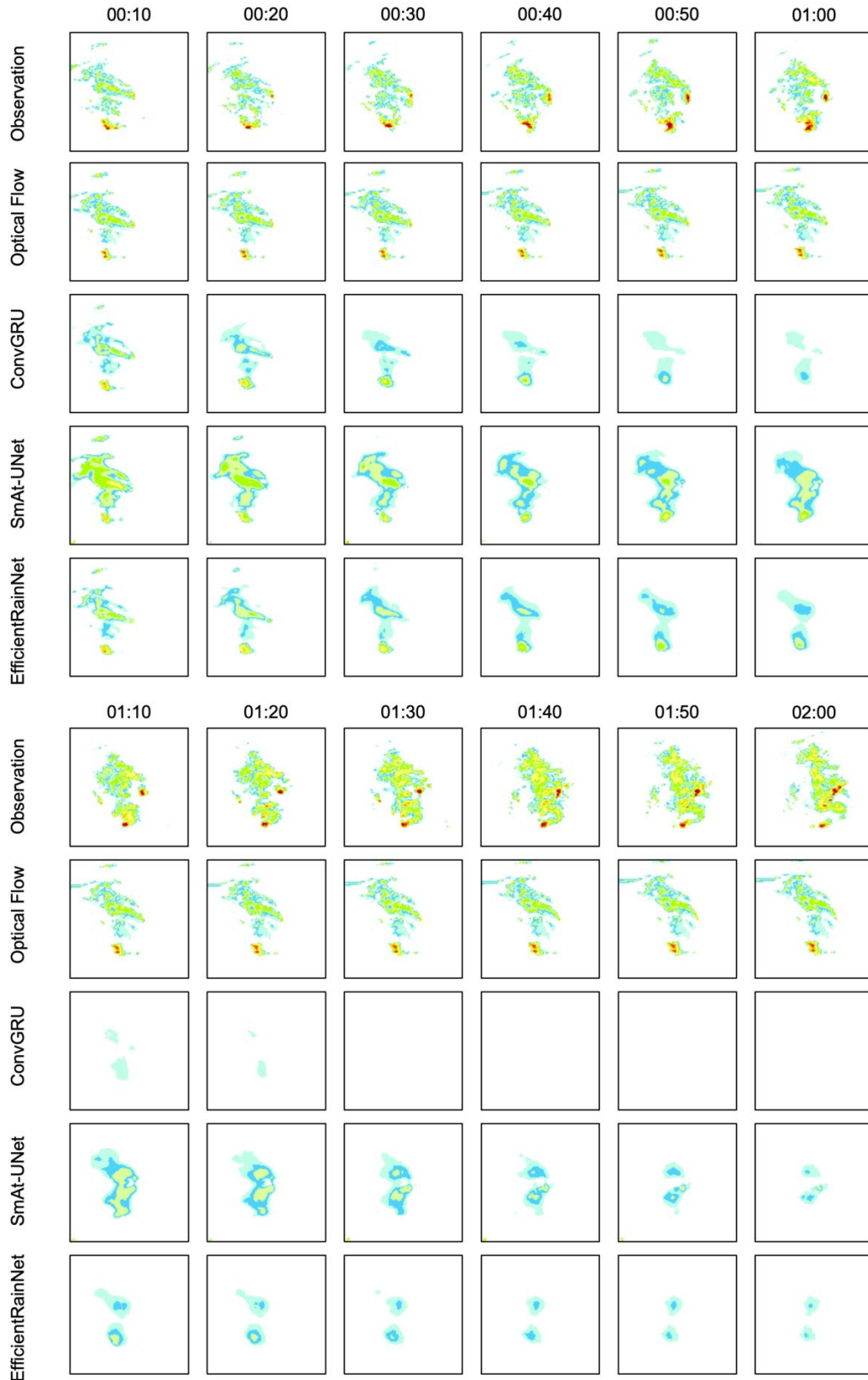


Figure A1. Forecast visualization for all methods for a rainfall event from the test dataset

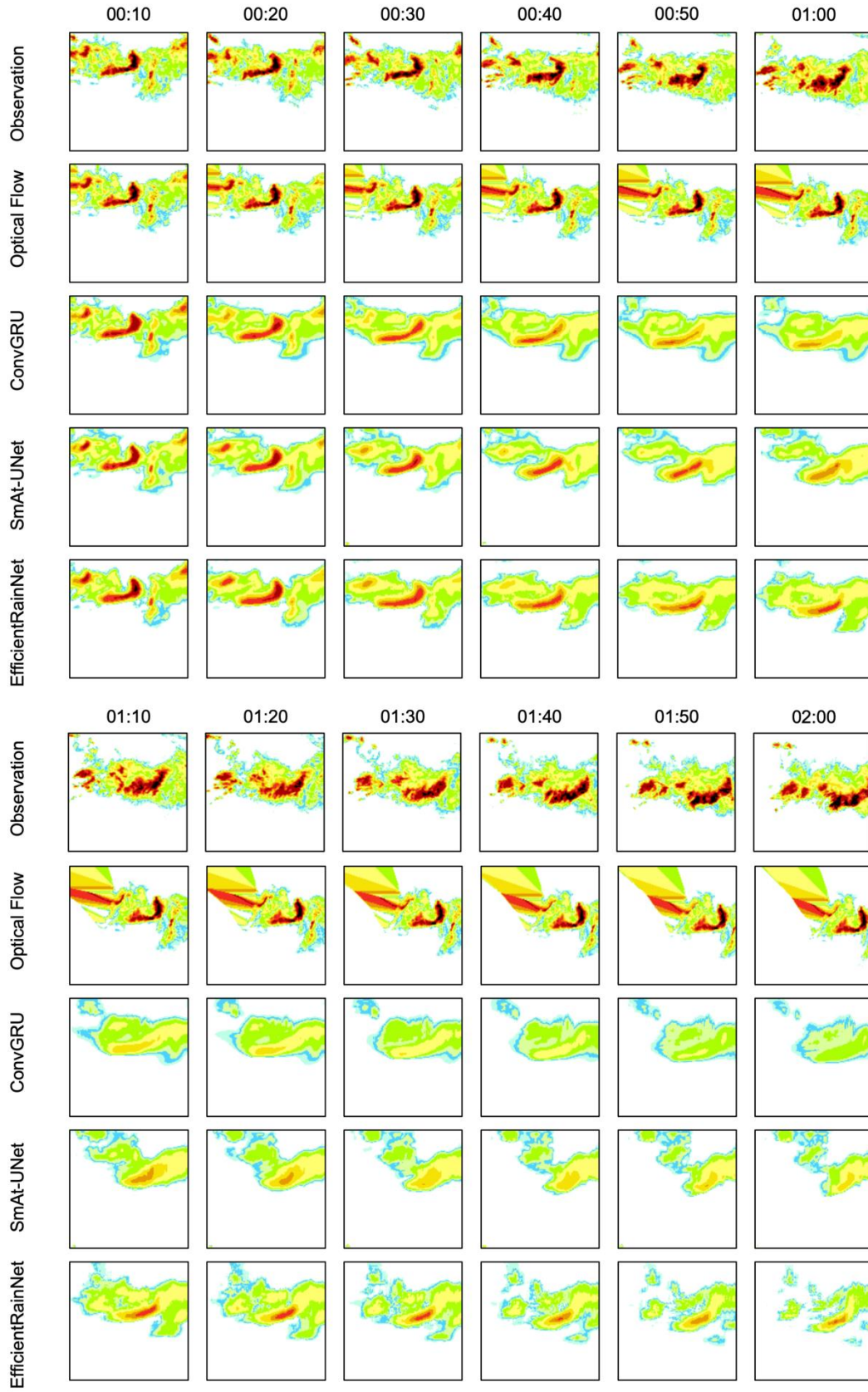


Figure A2. Forecast visualization for all methods for a rainfall event from the test dataset

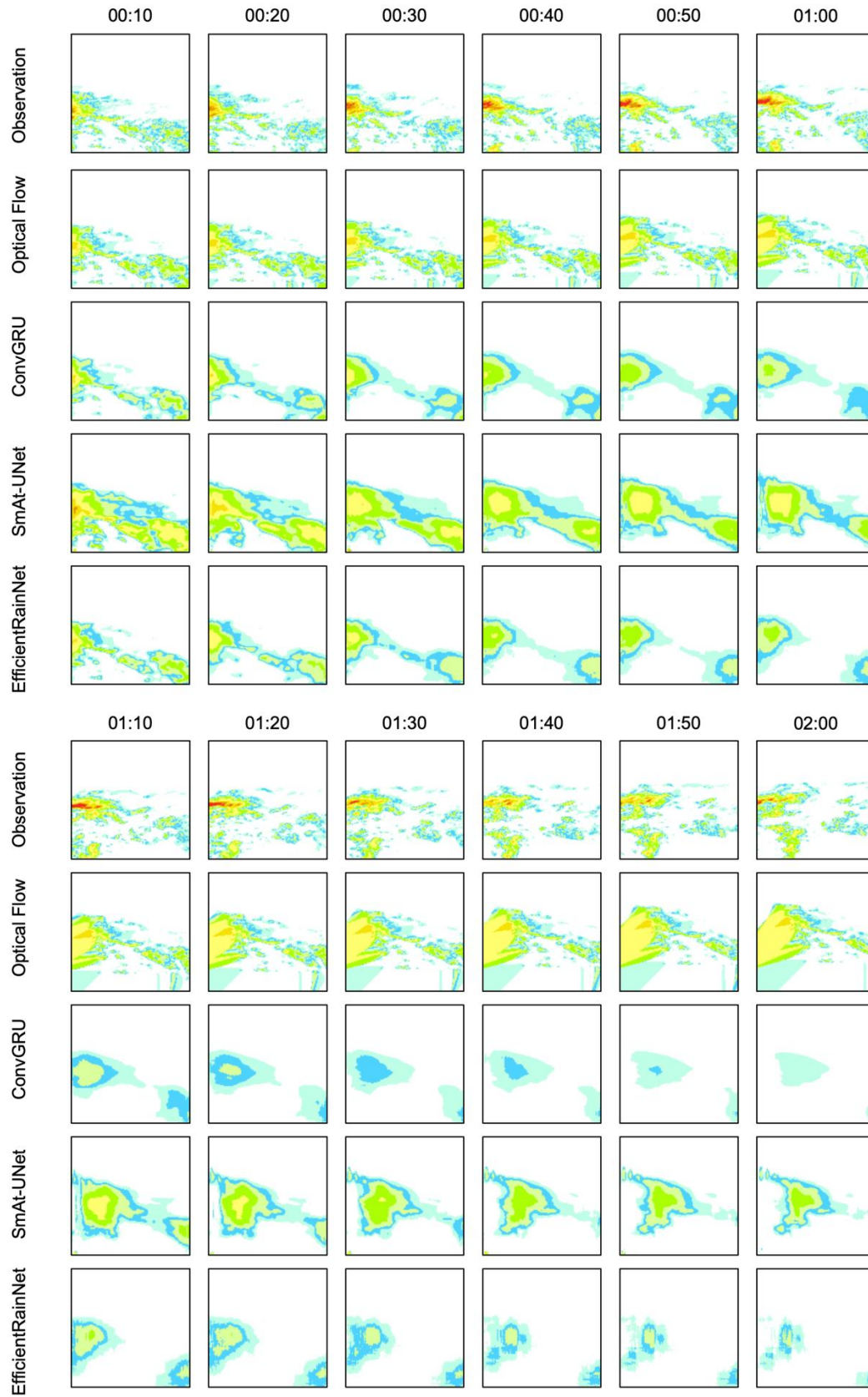


Figure A3. Forecast visualization for all methods for a rainfall event from the test dataset